Advanced LIGO: The next generation of gravitational wave detectors

Gregory M Harry for the LIGO Scientific Collaboration

LIGO Laboratory, Massachusetts Institute of Technology, 175 Albany Street, Cambridge, Massachusetts, 02139

E-mail: gharry@ligo.mit.edu

Abstract. The Advanced LIGO gravitational wave detectors are next generation instruments which will replace the existing initial LIGO detectors and are currently being constructed and installed. Advanced LIGO strain sensitivity is designed to be about a factor 10 better than initial LIGO over a broad band and usable to 10 Hz, in contrast to 40 Hz for initial LIGO. This is expected to allow for detections and significant astrophysics in most categories of gravitational waves. To achieve this sensitivity, all hardware subsystems are being replaced with improvements. Designs and expected performance are presented for the seismic isolation, suspensions, optics, and laser subsystems. Possible enhancements to Advanced LIGO, either to resolve problems that may arise and/or to allow for improved performance, are now being researched. Some of these enhancements are discussed along with some potential technology being considered for detectors beyond Advanced LIGO.

1. Overview

The Laser Interferometer Gravitational-wave Observatory (LIGO) project was envisioned from inception to follow up the initial detectors with improved instruments. The initial LIGO detectors reached their design sensitivity in 2006 [1] and have produced astrophysically interesting results [2]. Advanced LIGO is the name given to the next generation of detectors that will use the existing vacuum envelopes at the two LIGO sites in Louisiana and Washington state (See Figure 1). These new detectors will include improved seismic isolation, suspensions, optics, lasers, and all other hardware subsystems. US National Science Foundation funding for Advanced LIGO construction and installation began in April 2008. Installation of hardware is planned to be underway in early 2011 and first observations could begin as early as 2014.

1.1. Sensitivity

Advanced LIGO will consist of three interferometers, two at Hanford, WA and one at Livingston, LA. Each detector will be a Michelson interferometer with two perpendicular Fabry-Perot cavity arms 4 km long. This represents a change from the initial LIGO design, where one of the Hanford interferometers had 2 km long arms. There will be power recycling cavities to increase optical power as was the case for the initial detectors. In addition, there will be signal recycling cavities [3] which will allow for tuning of the quantum noise contribution to the total noise. This will enhance sensitivity at some frequencies at the expense of others. The baseline design is to have all three interferometers in a signal recycling configuration that gives good sensitivity across a wide band centered around 100 Hz. Other tunings may be chosen initially or in later

Figure 1. The LIGO sites in Livingston, Louisiana (left) and Hanford, Washington (right). The arms extend 4 km from the corner station and contain vacuum pipes so the entire optical path is in vacuum.

configurations as determined by the astrophysical opportunities and instrumental constraints. For instance, a narrowband mode with enhanced sensitivity at a likely pulsar frequency (perhaps around 600 Hz [4]) while having higher noise at other frequencies could be implemented in a later phase. The arm length difference at the dark port of the interferometer will be read out using homodyne detection [5]. Gravitational wave signals will thus be measured as amplitude modulations of the light at their actual frequency. This is in contrast to initial LIGO, where synchronous modulation-demodulation was used for the gravitational wave readout. Homodyne detection will eliminate technical noise associated with the modulation and demodulation, but will require an additional output mode cleaner immediately before the readout photodiodes. The optical layout of Advanced LIGO, showing the Michelson configuration, the Fabry-Perot arms, the power and signal recycling cavities, and the output mode cleaner, is shown in Figure 2.

Advanced LIGO is designed to have about an order of magnitude better sensitivity in its most sensitive band compared to initial LIGO. This will mean a strain noise of $3 \times 10^{-24}/\sqrt{\text{Hz}}$ in the most sensitive band, but a goal is to have as much as a factor of three improvement beyond this level over a 100 Hz band. The bandwidth of Advanced LIGO is also designed to be wider, going down to 10 Hz. The goal for duty cycle is to have all three detectors operating 75 % of the time, which was achieved individually by two of the three initial LIGO detectors [1]. No specific goal is set for non-Gaussian noise, but the aim is to reduce the rate of spurious noise glitches below the initial LIGO level, as this was a significant limitation to burst and inspiral searches.

Figure 3 shows the principal noise sources for a single Advanced LIGO interferometer. At very low frequencies, below 10 Hz, seismic noise, environmental disturbances, and technical noise sources will dominate. At low frequencies, between 10 and about 40 Hz, radiation pressure noise, thermal noise from the suspensions, and possibly gravity gradient noise [6] will be the limiting sources. At intermediate frequencies, between 40 and 200 Hz, thermal noise from the mirror optical coatings and combined quantum effects from the light will set the limit. Above 200 Hz, shot noise from the light will dominate. These noise levels are expected to be above the limits set by the facilities which are due to phase noise from residual gas in a 10^{-9} torr vacuum and from gravity gradients, although at low frequencies the gravity gradient noise may come close to the Advanced LIGO noise level. The hardware that is designed to reach this sensitivity is discussed in detail in Section 2 below.

1.2. Astrophysics

With improved noise levels over initial LIGO, Advanced LIGO will have greater sensitivity to a wide range of astrophysical gravitational waves. The factor of 10 improvement in noise will

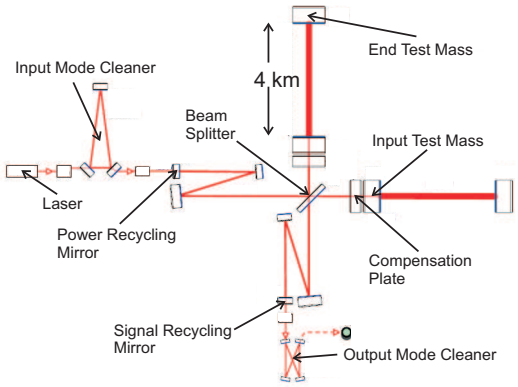

Figure 2. Advanced LIGO optical layout. Light travels from the laser through the input mode cleaner into the power recycling cavity. The light is split at the beamsplitter, then enters the two 4 km long arm cavities formed by the input and end test masses. Any signal exits through the signal recycling mirror and output mode cleaner. Also shown are the compensation plates used to control thermal lensing.

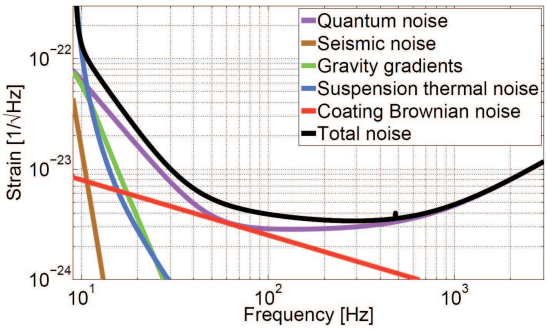

Figure 3. Anticipated contributions from individual noise sources to the total Advanced LIGO sensitivity (black). Noise sources shown are seismic noise (brown), suspension thermal noise (blue), coating thermal noise (red), gravity gradient (green) and quantum noise from the light (purple).

result in 1000 times the volume of space that can be searched for those sources in the mid-band of Advanced LIGO. These sources would include unmodeled bursts where the details and even nature of sources is not known. This could include supernovas, compact object mergers, neutron star instabilities, and cusps in cosmic strings. Searches for inspirals of neutron stars and/or black holes will also be possible over a greater volume than initial LIGO. An individual interferometer will have a direction and source averaged [7] range to binary neutron stars inspirals of around 200 Mpc. This is expected to be sufficient to see up to 40 neutron star inspiral events per year [8]. The equivalent expectation for 10 $M_\odot$ black hole binaries is 30 per year, and 10 per year for mixed neutron star-black hole inspirals. The final two estimates have far greater uncertainty than the first due to less information about populations. Advanced LIGO will also be able to observe in the previously inaccessible 10-40 Hz band, allowing longer measurements of light objects such as neutron stars, and the ability to observe signals before coalescence of far more massive objects in the hundreds of solar mass range.

With two years of data at the Advanced LIGO sensitivity, there are several low mass X-ray binaries that possibly could be detected from their output of continuous gravitational waves. There could also be pulsars or other sources that are not known electromagnetically but might be seen gravitationally with Advanced LIGO. For a gravitational stochastic background, an energy density of 10^{-9} times the Universe's closure density will be within reach using just 3 months of Advanced LIGO data. This will improve as the square root of observation time. At this level there are predictions of stochastic gravitational waves from early universe phase transitions [9] and some predictions for more exotic sources of a broadband gravitational wave background [10].

Advanced LIGO will also participate in multimessenger astronomy, adding detections of gravitational waves to neutrino and gamma-ray burst observations. Simultaneous detections with neutrinos could reveal information about the processes happening deep inside supernovas. The detection of gravitational waves from compact object mergers in coincidence with a short

gamma ray burst would provide direct evidence for the compact binary progenitor model [11]. The LIGO collaboration is making plans with other collaborations that run neutrino, gamma ray, and other detectors so that during Advanced LIGO operation the full potential of multimessenger astronomy will be realized.

2. Hardware

2.1. Seismic Isolation

The Advanced LIGO seismic isolation subsystem is designed to provide a quiet and controlled platform in all six degrees of freedom from which the test masses and other optics can be supported. In addition, it will provide low frequency, relatively large distance ($\sim$ 1 mm), positioning of all optics. There are two separate designs for the Advanced LIGO seismic isolation; a large chamber design for the test masses and beamsplitters that allows the optics to hang below, and a small chamber design for additional optics where the optics rest on top. The description here will focus on the large chamber isolation as this is what will reduce contributions to the test mass noise.

The Advanced LIGO test masses must be held in place to within 10^{-14} m by the seismic isolation and suspension subsystems combined. Much of the roughly 1 μm RMS motion of the ground comes at frequencies below about 10 Hz from seismic and other disturbances. The test masses must therefore be isolated from these environmental disturbances. The seismic isolation subsystem will provide about a factor of 10 isolation at the microseism peak frequency ($\approx$ 0.15 Hz) and a factor of about 1000 in the 1-10 Hz band, with the balance of the isolation coming from the suspension subsystem. At frequencies greater than roughly 10 Hz the ground noise is sufficiently small that the isolation targeted at lower frequency noise is sufficient. The total isolation is provided by a stage external to the vacuum, a two-stage, in-vacuum active isolation platform, and the test mass suspensions. The suspensions will be discussed in Subsection 2.2 while the other stages are discussed here.

External to the vacuum chambers is a hydraulic actuation subsystem on both the large and small chambers. This subsystem is designed to provide $\pm$1 mm of positioning in all three displacement degrees of freedom and $\pm$1 mrad in the angular degrees of freedom. In addition, it provides isolation in the frequency band 0.1 to 5 Hz. This is all accomplished by having laminar-flow, low-velocity hydraulic actuators exerting up to 1800 N on support tubes which carry the internal seismic isolation subsystem and payload; bellows allow the motion to be transmitted into the vacuum chamber. The signals from an inertial and displacement sensor colocated with the actuator are blended to provide feedback to the actuators while seismometers on the ground provide feedforward to get additional performance at low frequency [12]. This will provide about a factor of 10 reduction in the amplitude of large seismic disturbances due to human activity (nearby automobile traffic, tree cutting, etc.) as well as displacements from Earth tides, ocean waves, seasonal changes in temperature and ground water level or other natural, large amplitude, low frequency effects. It also allows control authority to be offloaded from the in-vacuum subsystems, which reduces problems with heating and power supply noise. This hydraulic isolation subsystem was installed at the LIGO Livingston Observatory in 2004 and has been operational for the subsequent observations. In Advanced LIGO this hydraulic subsystem will be extended to Hanford.

The in-vacuum seismic subsystem provides isolation above about 0.2 Hz and consists of two-stages of platforms connected to each other by springs. Each stage is supported by 3 maraging (precipitation hardened) steel blade springs and short pendulums from the stage above it to provide vertical and horizontal compliance in 6 degrees of freedom. Contained in each stage are six position sensors and six seismometers which collectively measure motion in all six degrees of freedom. The signals from these detectors are fed back to magnetic actuators to reduce the motion of the platforms. The rigid body modes of these stages are between 1.3 and 7 Hz, while

the unity gain frequency of the control loop will be about 25 Hz. Together, these stages provide isolation of about a factor of 300 at 1 Hz and about 3000 at 10 Hz, in amplitude. The second stage contains an optical table, from which the suspension and test mass are supported.

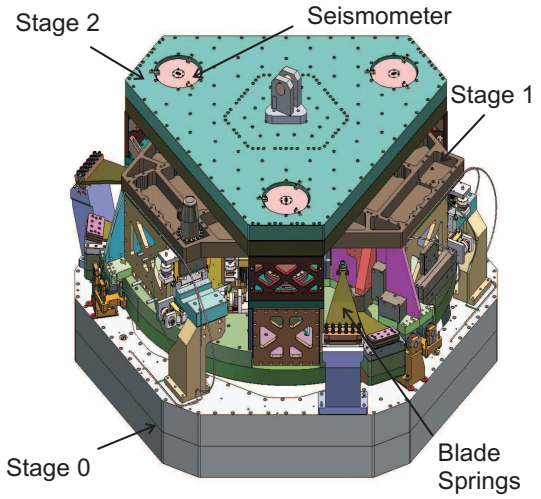

Figure 4. Internal stages of the large chamber seismic isolation subsystem. The hydraulic actuators support tubes outside the vacuum which cross into the vacuum tanks and support Stage 0 of the internal isolation. Stage 1 is supported from Stage 0 by the maraging steel blade springs, as is Stage 2 from Stage 1. A vertical seismometer in Stage 2 is also shown.

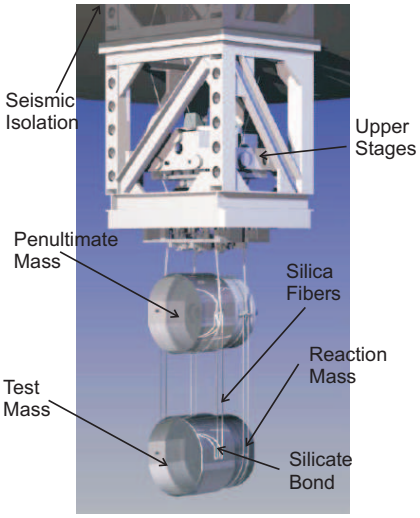

Figure 5. Advanced LIGO suspension. The test mass is at the bottom connected to the penultimate mass above it with silica fibers. The fibers are welded to silica attachment blocks which are silicate bonded to the masses. Above the penultimate mass are the upper two stages made of metal. The reaction mass behind the test mass can also be seen.

2.2. Suspensions

The Advanced LIGO test masses will be supported by suspensions that hang below the seismic isolation platforms. These suspensions are multistage pendulums with a final stage consisting of the test mass hanging on fused silica fibers. This provides additional passive isolation, allows for necessary control forces to be applied without adding excess noise, and minimizes the effect of thermal noise. This design is based on the suspensions in the GEO 600 interferometer [13]. The same groups in the United Kingdom, led by the University of Glasgow, responsible for those in GEO 600 have designed and are contributing the Advanced LIGO test mass suspensions. To meet the more stringent performance requirements of Advanced LIGO, a four-stage pendulum design, as opposed to the three-stage design used in GEO 600, has been developed.

The top mass of the suspension is suspended by two steel wires connected to two cantilever-mounted, pre-curved spring blades made from Marval 18 (18% Ni) maraging steel. The second of the four masses in the quadruple suspension is similarly held. These two top masses are made from metal, but the third mass is silica glass. It is suspended from cantilevers by steel wires that loop around its cylindrical shape. The final mass is the test mass of the interferometer, a 40 kg cylinder made of fused silica glass. Details of the test mass are discussed in Subsection 2.3. The test mass is connected to the penultimate mass solely by fused silica to reduce thermal noise.

Each stage of the pendulum provides isolation that falls off as f^{-2} above its pendulum frequency. These resonances are chosen to be between 0.4 Hz and 4 Hz, with the exception of

the highest vertical and roll modes. Thus thermal and other noise sources from higher in the chain are greatly reduced before affecting the test mass. The test mass has the least isolation from the final pendulum stage, this is the reason everything below the penultimate mass is made from low mechanical loss fused silica rather than metal. The sides of both the test mass and the penultimate mass will have silica attachment blocks connected to them by silicate bonding [14]. A silicate bond has greater mechanical loss than silica, but the area of the bond and its distance from the laser readout on the test mass are such that this excess loss will not noticeably increase the thermal noise. Four fused silica fibers 400 μm in diameter and 60 cm in length are welded to these ears to connect the two masses together. Note that circular cross section fibers have replaced the rectangular cross section ribbons which were in preliminary Advanced LIGO designs because of fabrication challenges, without any sacrifice in noise [16]. The diameter of the silica fibers is chosen so the stress will be about 1/3 of the breaking strength and the length is as long as possible (to give a low pendulum frequency) consistent with keeping the violin mode frequencies high enough for control purposes. The fibers have a "dumbbell" shape [17] with thicker ends whose diameter is chosen to minimize thermoelastic noise [15], while the long thin central region ensures the violin mode frequencies are high and the highest vertical bounce mode is low. The thermal noise expected from this suspension will be below the level of the radiation pressure noise from the light in the normal operating mode of Advanced LIGO, see Figure 3. However, to optimize the sensitivity for low frequency sources, the laser power can be lowered to reduce radiation pressure. This will make the suspension thermal noise, along with gravity gradient noise, the limiting noise sources between 10 and about 40 Hz.

In addition to the main quadruple suspension chain that supports the test mass, there will also be a nearly identical reaction chain placed 5 mm behind it. This chain will allow control forces for global angular and longitudinal degrees of freedom to be applied from a quiet platform. These forces will be applied hierarchically, with large forces applied with coils and magnets between both the upper intermediate and penultimate masses but with fine control forces applied with an electrostatic drive (ESD). The ESD is a gold pattern deposited on the face of the final reaction mass and applies forces to the test mass with an electrostatic field. It may have other uses as well, including damping parametric instabilities and sensing charge buildup (see Section 3). Local damping of all the low frequency suspension modes will be done with co-located sensors and actuators on the top mass to insure that any sensing noise will be well isolated from the test mass.

2.3. Optics

The Advanced LIGO optics will direct and control the light used to read out the position of the test masses. The test masses themselves are optics with stringent requirements on size, scatter, absorption, and thermal noise. Other optics include the beamsplitter, the power and signal recycling mirrors, input optics including the input mode cleaner and mode matching telescope, as well as auxiliary optics including those used for thermal compensation of the test masses.

The test masses are 40 kilogram silica optics, 34 cm in diameter and 20 cm thick, used at both the inputs and ends of the 4 kilometer Fabry-Perot cavities. They are supported by the suspension subsystem below the seismic isolation and are chosen to be the largest size that is practical to both make and support. This large size reduces the radiation pressure noise. Fused silica glass was chosen for the test mass substrates over single crystal sapphire, which had been considered in preliminary designs. It was found that a complete instrument using silica can have roughly the same level of thermal noise, while there were concerns with both optical absorption and manufacturing issues in large crystals of sapphire.

The silica substrates are polished to a surface figure $\leq$0.3 nm RMS and a microroughness $\leq$0.16 nm RMS which are necessary to approach the goal of no more than 80 ppm total loss per round trip. They are polished to about 2 kilometer radii of curvature which creates a nearly

concentric cavity in the 4 km arms. This allows for large radii (6.2 cm on the end mirrors and 5.3 cm on the input mirrors) laser spots on the test masses, which reduces both coating and substrate thermal noise. These spot sizes are the largest practical while keeping optical losses from diffraction and control problems from angular instabilities [18] to a workable level.

The optical coatings on the test masses will be made of alternating layers of silica and 25% titania doped into tantala. Titania doped tantala has been shown to have lower mechanical loss, and thus lower thermal noise, than undoped tantala [19]. Titania-tantala also reduces the optical absorption down to 0.3-0.5 ppm, around a factor of 2 improvement over undoped tantala. The thickness of each coating layer is chosen so that three goals are met; the transmission at 1.064 μm, the main laser wavelength, is $\leq$ 6 ppm on the end mirrors and 1.4% on the input mirrors, the reflectivity at half the laser wavelength, 532 μm, is such that a lower-finesse secondary interferometer can be operating during lock acquisition, and the amount of the high index titania-tantala material is minimized to reduce coating thermal noise [19].

Even with very low absorption coatings and substrates, thermal lensing in the test masses will need to be compensated; we build on the experience in initial LIGO [20]. Thermal lensing is expected to be most problematic in the input test masses where the beam must transmit through the substrate and the high power of the Fabry-Perot cavity is experienced by the coating. The input test mass substrates will be made from Heraeus Suprasil 3001 fused silica, which is the lowest absorbing silica at 1.064 μm. To reduce the thermal gradient produced by the beam in the optic center, ring resistance heaters will be installed surrounding the input test masses. They are designed to heat the barrel of the optic radiatively. This is complemented with a flexible system based on a carbon dioxide laser projected onto the reaction masses behind the input test masses (called compensation plates because of this use, see Figure 2). This carbon dioxide laser subsystem is similar to the thermal compensation that was used in initial LIGO. The 10 μm light is readily absorbed by the silica substrates creating a heat pattern. The shape and intensity of the beam can be adjusted from outside the vacuum to respond to changing power levels in the interferometer, non-uniform and/or changing absorption in optics, and other changes to the thermal state. The compensation plates will have gold barrel coatings which will increase the efficiency of the thermal compensation by more evenly distributing the heat radially across the optic. Sensing of the thermal distortions in the optic will be via Hartmann sensors [21] developed and contributed with other hardware by The University of Adelaide and Australian National University. In addition, the power recycling cavities in Advanced LIGO will be stable, unlike the nearly unstable cavities in initial LIGO. This will be created by using a folded set of three mirrors, see Figure 2. A stable cavity allows the beam to be reduced in size on the recycling mirrors to minimize the sensitivity to thermal lenses in the input mirrors. In addition, RF sidebands, which are used for locking the interferometer, are resonant in the stable power recycling cavity and audio sidebands produced by gravitational waves resonate in the stable signal recycling cavity.

Another consideration stemming from high optical power is parametric instabilities [22]. Energy can be exchanged between the optical modes in the cavity and the acoustic modes of the test masses, which can lead to the test mass modes ringing up to high enough amplitude such that there are problems with control and eventually lock loss. Sensitivity to this phenomenon is exacerbated when the acoustic modes have high quality factors, which is typically the case with the low mechanical loss coatings and substrates that are needed for low thermal noise. To mitigate this, dampers tuned to frequencies in the range of the mirror normal modes (tens of kHz) that attach to the test masses are being considered. These would damp out problematic high frequency modes but would not significantly increase the lower frequency thermal noise. There are other approaches to dealing with this problem under development for possible inclusion in enhancements to Advanced LIGO that are discussed in Section 3.

Advanced LIGO optics other than the test masses still must satisfy strict optical requirements,

if not as strict as for the test masses. The input mode cleaner mirrors, the beam splitter, and the signal and power recycling mirrors are all made of low absorption fused silica, are coated with silica/tantala coatings for low optical loss, and polished so that they have less than a few hundred ppm of scatter. The input mode cleaner optics will experience the highest optical power densities of any optics in Advanced LIGO because of the smaller spot sizes on these optics. Other input optics, including a Faraday isolator and electro-optic modulators, must also be designed to handle high optical power.

2.4. Laser

The laser subsystem provides the light used for sensing the position of the test masses to the interferometer. The light will have a wavelength of 1.064 μm and come from a Nd:YAG-based laser developed and contributed by members of the GEO collaboration (Albert-Einstein-Institute and Laser Zentrum Hannover). This is the same team which developed the GEO 600 laser and the Advanced LIGO laser design [23] draws heavily on that experience.

To improve the sensitivity limit from shot noise, the amount of light delivered to the interferometer needs to be increased over what was available in initial LIGO. The signal-to-noise ratio in the shot noise dominated regime goes as $1/\sqrt{P}$, where P is the optical power, so the laser power is being increased from about 10 W in initial LIGO to 180 W in Advanced LIGO. It is because of this increase in power that the backreaction on the test masses via radiation pressure, whose signal-to-noise ratio scales as $\sqrt{P}$, is a significant low-frequency noise contributor. This fundamental tradeoff between shot noise and radiation pressure noise is characteristic of a Heisenberg microscope. Advanced LIGO will be a macroscopic realization of this quantum limited device. The signal recycling mirror allows the Advanced LIGO sensitivity to exceed the standard quantum limit, which is determined by the quantum uncertainty of the test masses, in a limited bandwidth by coupling position and momentum uncertainties [24]. This is done at the expense of sensitivity at other bands.

To achieve this high power, the Advanced LIGO laser is designed with three stages; the first is a non-planar ring oscillator (NPRO) that generates a 2 W beam, the second is an amplifier which boosts the optical power to 35 W and acts as the master laser to the third stage, which is an injection locked ring oscillator that increases the optical power to 180 W. The first two stages, with a power of 35 W, are being used as the light source in the final data runs with the initial LIGO interferometers. These lasers have been successfully in operation during both data taking and commissioning since April of 2008.

The laser subsystem also provides pre-stabilization and filtering of the laser frequency, the spatial profile of the beam, the laser direction pointing, and fluctuations in the optical power. A frequency reference is provided by a cavity like what is done in initial LIGO. The reference cavity is made from monolithic fused silica and is both thermally and seismically isolated from external disturbances. Signals from this cavity are fed back to an electro-optic modulator for phase corrections, as well as to the NPRO cavity length and temperature controls. The beam's spatial profile and pointing is filtered by a longer pre-mode cleaner (PMC) than is used in initial LIGO. The PMC is a bowtie cavity in series with the laser that has a round trip length of 2 m, a finesse of 124, and circulating power of 9 kW. The PMC also reduces higher order TEM modes and provides filtering of power noise at radio frequencies. Power stabilization at lower frequencies will either be applied with an acousto-optic modulator on the 2 W beam after the NPRO or on the 180 W beam leaving the third stage.

3. Enhanced Advanced LIGO and Third Generation

Research is progressing on possible enhancements to Advanced LIGO. There are research efforts in optics, seismic isolation, and light sources to provide additional sensitivity beyond the baseline Advanced LIGO level. In optics, there are multiple research directions aimed at improving the

coating thermal noise since it is expected to be a limiting noise source in the most sensitive band of Advanced LIGO. Trying to find coating materials with lower mechanical loss, and trying to understand the sources of mechanical loss in existing coating materials is a major effort [25]. Another approach is to increase the effective beam spot size without increasing diffraction losses by using differently shaped optical beams in the interferometer, including mesa [26] and higher order Gauss-Laguerre [27]. Many of these improvements would require new optics, but the potential payoffs are so significant that this is not ruled out. To reduce both shot and radiation pressure noise, the use of light squeezed into non-classical states is under development [28]. Most of the major aspects of squeezing have been demonstrated in the laboratory and on prototypes, and there are plans being considered for testing squeezed light on a full LIGO interferometer just prior to Advanced LIGO installation.

There is also laboratory research aimed at technical noises that may prevent Advanced LIGO from reaching its sensitivity goals. One concern is with electrical charge buildup on the test masses. The baseline design includes silica-tipped earthquake stops as an improvement over the viton-tipped ones used in initial LIGO. These viton tips showed evidence of transferring charge to the optics which then caused excess noise [29]. If this proves insufficient, there are charge mitigation subsystems utilizing UV light and/or low energy ions that are being developed and tested [30]. Parametric instability [22] is another area of potential concern. In addition to the damping system mentioned in Section 2.3, it may be possible to use the electrostatic drive in a feedback loop to damp the high frequency ($\geq$10 kHz) modes susceptible to parametric instabilities. There is research, as well, on injecting light into the interferometer tuned to cancel higher order optical modes that can contribute to parametric instability [31]. If disturbances from the environment create excess noise at low frequencies, this could be addressed through seismic platform interferometers [32]. This would be a series of interferometers that lock together the seismic isolation stages which would greatly reduce differential motion between optics in different vacuum chambers. There is also ongoing research on understanding possible mechanisms for non-Gaussian creep noise in crucial materials, notably the maraging steel blades [33], the silicate bonds in the suspensions, as well as coating materials. This could be important should non-Gaussian noise prove a major limitation on Advanced LIGO sensitivity.

There is also longer term research looking at hardware improvements beyond Advanced LIGO. At low frequencies, building an interferometer underground as a way to reduce gravity gradient noise is being explored [34]. Diffractive optics, which would eliminate the need for the light to transmit through optics, is being researched [35] as a way to allow for very high optical powers. In addition to ongoing materials and beam shaping work, the possibility of using cavities for end mirrors [36], corner reflectors [37], or Brewster angle mirrors [38] is being investigated to reduce or eliminate the need for optical coatings. This has the potential to greatly reduce thermal noise in the midfrequency band. Further reductions in thermal noise from both the test masses and the suspensions may be possible in some frequency bands with materials like sapphire or silicon [39] and/or by cooling the interferometer to cryogenic temperature [40]. Many of these technologies are just beginning to be considered and have yet to be demonstrated as practical for an actual gravitational wave detector.

Acknowledgments
The authors gratefully acknowledge the support of the United States National Science Foundation for the construction and operation of the LIGO Laboratory and the Science and Technology Facilities Council of the United Kingdom, the Max-Planck-Society, and the State of Niedersachsen/Germany for support of the construction and operation of the GEO600 detector. The authors also gratefully acknowledge the support of the research by these agencies and by the Australian Research Council, the Council of Scientific and Industrial Research of India, the Istituto Nazionale di Fisica Nucleare of Italy, the Spanish Ministerio de Educación y Ciencia,

the Conselleria d'Economia, Hisenda i Innovació of the Govern de les Illes Balears, the Royal Society, the Scottish Funding Council, the Scottish Universities Physics Alliance, The National Aeronautics and Space Administration, the Carnegie Trust, the Leverhulme Trust, the David and Lucile Packard Foundation, the Research Corporation, and the Alfred P. Sloan Foundation. This paper has been assigned LIGO Document Number LIGO-P0900255.

References

[1] B. Abbott *et al.*, Reports on Progress in Physics **72** (2009) 076901.
[2] The LIGO Scientific Collaboration and the Virgo Collaboration, Nature **460** (2009) 990; B. P. Abbott *et al.*, The LIGO Scientific Collaboration, Physical Review D **79** (2009) 122001; B. P. Abbott *et al.*, The LIGO Scientific Collaboration, Physical Review Letters, **102** (2009) 111102; B. P. Abbott *et al.*, The LIGO Scientific Collaboration,The Astrophysical Journal Letters **701** (2009) L68.
[3] B. J. Meers, Physical Review D **38** (1988) 2317.
[4] J. S. Heyl, The Astrophysical Journal **574** (2002) L57.
[5] R. L. Ward *et al.*, Classical and Quantum Gravity **25** (2008) 114030.
[6] K. S. Thorne and C. J. Winstein, Physical Review D **60** (1999) 082001.
[7] K. S.Thorne, in *300 Years of Gravitation*, S. Hawking and W. Israel, (Cambridge University Press, 1987), 330.
[8] K. S. Thorne and C. Cutler, in *Proceedings of 16th International Conference on General Relativity and Gravitation*, N. T. Bishop and S. D. Maharaj, (World Scientific, Singapore, 2002), 72.
[9] R. Apreda *et al.*, Nuclear Physics B **631** (2002) 342.
[10] A. B. Buonanno, M. Maggiore, and C. Ungarelli, Physical Review D **55** (1997) 3330.
[11] B. Paczynski, Acta Astronomica **41** (1991) 257.
[12] B. Abbott, *et al.*, Classical and Quantum Gravity **21** (2004) S915.
[13] S. Hild for The LIGO Scientific Collaboration, Classical and Quantum Gravity **23** (2006) S643.
[14] P. H. Sneddon *et al.*, Classical and Quantum Gravity **20** (2003) 5025.
[15] G. Cagnoli and P. A. Willems, Physical Review B **65** (2002) 174111.
[16] A. Cumming *et al.*, Classical and Quantum Gravity **26** (2009) 215012.
[17] P. Willems, Physics Letters A **300** (2002) 162.
[18] J. A. Sidles and D. Sigg, Physics Letters A **354** (2006) 167.
[19] G. M. Harry *et al.*, Classical and Quantum Gravity **24** (2006) 405.
[20] S. J. Waldman for The LIGO Scientific Collaboration, Classical and Quantum Gravity **23** (2006) S653.
[21] A. Brooks, P. Veitch, J. Munch, and T. Kelly, General Relativity and Gravitation **37** (2005) 1575.
[22] V. B. Braginsky, S. E. Stringin, and S. P. Vyatchanin, Physics Letters A **287** (2001) 331.
[23] B. Wilke *et al.* Classical and Quantum Gravity **25** (2008) 4040.
[24] A. Buonanno and Y. Chen, Physical Review D **26** (2002) 042001.
[25] I. Martin *et al.*, Classical and Quantum Gravity **25** (2008) 055005.
[26] J. Agresti *et al.*, Journal of Physics: Conference Series **32** (2006) 301.
[27] S. Chelkowski, S. Hild, and A. Freise, Physical Review D **79** (2009) 122002.
[28] K. Goda *et al*, Optics Letters **33** (2008) 92.
[29] R. S. Amin, LIGO Technical Note G070572-00-R, available at admdbsrv.ligo.caltech.edu/dcc/.
[30] D. Ugolini, M. Girard, and G. M. Harry, Physics Letters A **372** (2008) 5741.
[31] L. Ju, D. G. Blair, C. Zhao, G. Gras, Z. Zhang, P. Barriga, H. Miao, Y. Finn, and L. Merril, Classical and Quantum Gravity **26** (2009) 015002.
[32] R. W. Drever and S. J. Augst, Classical and Quantum Gravity **19** (2002) 2005.
[33] N. Virdone, *et al.* Nuclear Instruments and Methods in Physics Research Section A **593** (2008) 597.
[34] J. Harms, R. DeSalvo, S. Dorsher, and V. Mandic, arXiv/0909.3341 (2009).
[35] A. Bunkowski *et al.* Optics Letters **29** (2004) 2342.
[36] F. Ya. Khalili, Physics Letters A **334** (2004) 67.
[37] V. B. Braginsky and S. P. Vyatchanin, Physics Letters A **324** (2004) 345.
[38] S. Goßler, J. Crumpston, K. McKenzie, C. M. Mow-Lowry, M. B. Gray, and D. E. McClelland, Physical Review D **76** (2007) 053810.
[39] S. Rowan *et al.* SPIE Proceedings **4856** (2003) 292.
[40] R. DeSalvo, Classical and Quantum Gravity **19** (2002) 2021.